

Emerging Relation Network and Task Embedding for Multi-Task Regression Problems

Jens Schreiber
 University of Kassel
 Wilhelmshöher Allee 71-73
 34121 Kassel
 Email: j.schreiber@uni-kassel.de

Bernhard Sick
 University of Kassel
 Wilhelmshöher Allee 71-73
 34121 Kassel
 Email: bsick@uni-kassel.de

Abstract—Multi-task learning (MTL) provides state-of-the-art results in many applications of computer vision and natural language processing. In contrast to single-task learning (STL), MTL allows for leveraging knowledge between related tasks improving prediction results on the main task (in contrast to an auxiliary task) or all tasks. However, there is a limited number of comparative studies on applying MTL architectures for regression and time series problems taking recent advances of MTL into account. An interesting, non-linear problem is the forecast of the expected power generation for renewable power plants. Therefore, this article provides a comparative study of the following recent and important MTL architectures: Hard parameter sharing (HPS), cross-stitch network (CSN), sluice network (SN). They are compared to a multi-layer perceptron (MLP) model of similar size in an STL setting. Additionally, we provide a simple, yet effective approach to model task specific information through an embedding layer in an MLP, referred to as task embedding. Further, we introduce a new MTL architecture named emerging relation network (ERN), which can be considered as an extension of the SN. For a solar power dataset, the task embedding achieves the best mean improvement with 14.9%. The mean improvement of the ERN and the SN on the solar dataset is of similar magnitude with 14.7% and 14.8%. On a wind power dataset, only the ERN achieves a significant improvement of up to 7.7%. Results suggest that the ERN is beneficial when tasks are only loosely related and the prediction problem is more non-linear. Contrary, the proposed task embedding is advantageous when tasks are strongly correlated. Further, the task embedding provides an effective approach with reduced computational effort compared to other MTL architectures.

I. INTRODUCTION

A. Motivation

Multi-task learning (MTL) provides state-of-the-art results in many applications of computer vision and natural language processing (NLP) [1], [2], [3]. In contrast to single-task learning (STL), MTL allows for leveraging knowledge between related tasks improving forecast results on the main task (in contrast to an auxiliary task) or all tasks. Simultaneously, learning multiple tasks increases the sample size and allows learning a more general representation [1], which in contrast to STL, improves the forecast error. Further, they typically reduce the computational effort.

Even though there are several articles evaluating the effectiveness of MTL approaches for computer vision and NLP problems, there is a limited number of comparative studies

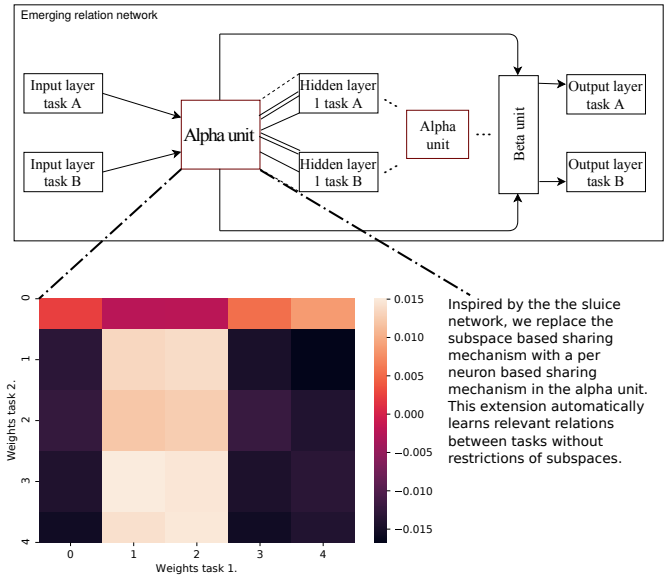


Fig. 1: Schematic overview of the proposed emerging relation network. The network replaces the subspace based sharing mechanism of the sluice network with a per neuron based sharing mechanism in the alpha unit. Outputs of the alpha units are concatenated through skip layers, for each task and layer, as input to the beta unit, providing task specific forecasts. Different line types refer to (potential) different relations automatically emerged during training. Those different sharing mechanisms are present in the exemplary heatmap of weights. In the heatmap, it is noticeable that one group has negative weights; another group has positive weights, while others are around zero.

on applying MTL architectures for regression and time series problems taking recent advances of MTL into account.

One challenging prediction problem is the forecast of the expected power generation for renewable power plants. Typically, predicting power generation is a two step approach. The first step involves forecasting the weather features, such as wind speed or radiation, with a time step of up to 72h in the future. These forecasts from so-called numerical weather prediction (NWP) are the input to the second step. In this step,

weather features are mapped as a regression problem to the generated power of a solar or wind farm. Overall, the process of forecasting the generated power, including the NWP, is often considered a non-linear time series problem [4], [5].

One problem is that the weather forecasts uncertainty increases with an increasing forecast horizon. Further, relations between different weather features, such as wind speed and air pressure, and between weather features and power generation, are non-linear. Predicting the generated power is limited by the local weather information from the NWP. However, an increased interest in renewable energy [6] requires improved forecasts to maintain a stable power grid and for trading, while reducing the computational effort at the same time [7]. As MTL allows making use of information from other wind and solar parks, it allows reducing (local) uncertainty from weather predictions for a single park and decreases the forecast error, respectively. It also reduces the computational effort.

This article provides a comparative study of recent advances in MTL for regression problems with an exemplary use-case in renewable energy.

B. Main Contribution

Therefore, this article provides a comparative study of the following recent and important MTL architectures: Hard parameter sharing (HPS), cross-stitch network (CSN), and sluice network (SN) by comparing it to a multi-layer perceptron (MLP) model of similar size in an STL setting¹. Further, we introduce **emerging relation network (ERN)** that replace the subspace based sharing mechanism of SNs with a per neuron based sharing mechanism in the **alpha unit**. This novel alpha unit allows the learning procedure to emerge relations automatically without a selection of the subspace hyperparameter. Fig. 1 gives the a schematic overview of the ERN. It also includes an example showing that relations and groups of relations emerge from the learning procedure, as highlighted in the heatmap of learned weights.

Additionally, we suggest a simple yet effective approach to model task specific information through an embedding layer in an MLP, referred to as **task embedding**, see Fig. 2. Training and evaluating on a solar and a wind park dataset yields to the following significant results against the STL MLP baseline:

- For the solar dataset, the task embedding achieves the best mean improvement,
- the mean improvement of the ERN and the SN are of similar magnitude.
- On the wind dataset, only the ERN achieves a significant improvement.
- Results suggest that the ERN is beneficial when tasks are only loosely related, and the prediction problem is more non-linear.

The remainder of this article is structured as follows. In Sec. II we detail related work. Sec. III outlines relevant deep learning architectures. Sec. IV describes the experimental

design and evaluation results with respect to the STL baseline. Finally, we conclude our work and propose future work in Sec. V.

II. RELATED WORK

In the following section, we summarize MTL in the field of deep learning, with a focus on computer vision and NLP. We limit the related work to approaches where the network learns the amount of joint and shared knowledge automatically. Then in the next section, we detail related work for multi-task regression problems. We outline the limited utilization of deep learning methods in this area in general and its current focus on HPS MTL architecture types.

A. Deep Learning Based Multi-Task Learning

In [1], an overview of novel methods in deep learning based MTL is given, including their work on SN. The SN is based on the CSN introduced in [2]. The CSN learns a combination of task specific and universal representations through a linear combination for computer vision problems. The SN introduced in [3] generalizes this idea by making use of skip layers and additional subspaces (with separate weights). The additional subspaces provide a more fine-tuned separation between common and task specific sharing achieving excellent results in NLP.

The formerly mentioned methods automatically learn what to share. Approaches such as the deep relation networks [8] require an at least partly pre-defined structure of the network. In [8], several task specific layers follow some joint convolutional layers. However, a prior to the separate layers allows them to automatically learn what to share, achieving good results for computer vision problems. Primarily, the network is considered an HPS architecture. The authors of [9] use a greedy learning approach to dynamically create branches for task specific and joint layers for computer vision problems. In [10] and [11], they focus on finding hierarchical network structures for NLP problems. The article [12] introduces an approach for automatic weighting different tasks during training based on the uncertainty of a task. This approach adds additional complexity to the training process and is not related to a specific architecture type that we are interested in.

B. Multi-Task Learning for Regression Problems

As stated before, there is limited research on using deep learning architectures for multi-task regression problems. In this section, we summarize articles in this area, for a detailed overview, refer to [1], [13]. In several articles, the utilization of Gaussian processes models commonalities through an equal prior on the parameters of the Gaussian processes, [14], [15], [16], [17]. Other works make use of linear models modeling the relationship between related tasks, [18], [19], [20]. These models are computationally efficient but cannot model non-linear relationships between tasks. In [21], the authors aim at modeling complex relations through shared weights of a least-squared support-vector regression. In particular, the authors use this approach to predict heat, cooling, and gas loads.

¹Source code is available under https://git.ies.uni-kassel.de/mtl_regression/ern_and_te_for_mtl_regression_problems.

The above articles disregard the capabilities of neural networks to learn shared knowledge automatically during training. In contrast, the authors of [22] combine knowledge from different network types through a fully connected neural network. In their goal to predict train delays, they have various kinds of data types. Therefore, the different data types are handled initially by either a long-term-short memory, an MLP, or a convolutional network. An MLP combines the extracted knowledge from those networks to forecast the train delays.

The article [23] proposes an MTL long short term memory network to forecast gas detection and concentration estimation of an intelligent electric sensing device simultaneously. Finally, [24] aims at predicting wind power ramps. To make the best use of sparse data from different wind parks, [23] combines the knowledge through an HPS network. Further, an adapted Adam optimizer takes care of imbalanced data.

The article [25] gives good insights and excellent results in the utilization of MTL architectures in a transfer learning setting with HPS networks. The authors also include a Bayesian variant of the proposed task embedding architecture. However, the Bayesian variant adds additional complexity compared to our proposed approach and results are solely evaluated in the transfer learning setting.

The literature review shows that most of the work for multi-task regression models are either focusing on models without neural networks or are utilizing HPS networks. However, articles from the domain of computer vision and NLP show noticeable results utilizing different types of HPS and soft parameter sharing (SPS) architectures.

III. METHODS

Typically in MTL, we differentiate between HPS and SPS architectures. Therefore, in Sec. III-A we give details on HPS, and in Sec. III-B we propose a simple task encoding approach for MLPs in MTL problems. While this approach is considered an HPS architecture, Sec. III-C and III-D introduce two recent advances from the fields of SPS. In Sec. III-D, we introduce our novel approach ERN.

A. Hard Parameter Sharing

HPS networks are architectures, where several hidden layers learn a shared representation for all tasks. Additional task specific layers allow transferring knowledge from this representation to the task specific problem.

B. MLP with Task ID Embedding

Fig. 2 depicts our own approach for MTL utilizing an MLP and an embedding layer. Primarily, this approach is inspired by so-called word embeddings from the NLP domain. In the NLP domain, word embeddings provide a continuous vector representation from a bag of words. The encoding through the embedding layer is learned, e.g., during a supervised training for sentiment classification. In the end, after training, similar words, such as queen and king, have a similar representation, while not related words are far away from each other in the encoded representation. In the context of renewable energy, the

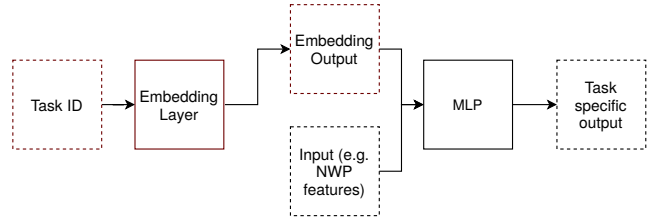


Fig. 2: Task embedding for MLP to create task specific predictions based on an hard parameter sharing architecture without separate layers. By encoding a task ID, for each task, through an embedding layer, the mlp learns task specific forecasts, while utilizing the data from all tasks to improve forecasts.

similarity is, e.g., given when two wind parks have a similar mapping between wind speed and the generated power.

In the MTL setting, we create a task ID for each task, additionally to other features. This task ID is the input to the embedding layer to encode task specific information. The encoded task information is concatenated with other features from the NWP as input to the MLP. The input layer for other features stays the same for all tasks. During the supervised training, to forecast the generated power, the network learns (through backpropagation) the encoding while making use of other features to create task specific forecasts.

As all tasks share the same layers, except the task ID encoding, this approach can be considered as an HPS network. In contrast to other HPS architectures, the task embedding architecture can reduce the number of parameters as it avoids additional separate layers. Naturally, through the combined training of all tasks, the architecture makes use of data augmentation. Ideally, the learned task encoding, allows the network to make use of samples from a task A for unknown weather situation in task B .

C. Cross-Stitch Network

In contrast to the previous two architectures, the CSN [2] is based on SPS. In SPS, each task has a separate network learning a separate representation for each task. In architectures such as CSN and SN, information between the different networks is shared by so-called **alpha units**, as also visualized in our own approach in Fig. 1. Alpha units allow sharing information through a linear combination from one task to another learned during training through backpropagation.

Equation (III-D) gives an *example for two tasks* A and B at layer $l \in 1, \dots, L - 1$:

$$\begin{bmatrix} \tilde{h}_{A,l}^T \\ \tilde{h}_{B,l}^T \end{bmatrix} = \begin{bmatrix} \alpha_{AA} & \alpha_{AB} \\ \alpha_{BA} & \alpha_{BB} \end{bmatrix} [h_{A,l}^T \quad h_{B,l}^T], \quad (1)$$

where the α matrix is of size $\mathbb{R}^{2 \times 2}$ for those tasks. The outputs $h_{A,l}$ and $h_{B,l}$ for the layer l are concatenated and multiplied by the respective alpha unit at this layer. The resulting linear combinations $\tilde{h}_{A,l}$ and $\tilde{h}_{B,l}$ are then utilized as input for the next layer of each task, similarly to Fig. 1. In

this example for task A and B , the final output is then given by $\tilde{h}_{A,L}^T$ and $\tilde{h}_{B,L}^T$.

D. Sluice Network

The authors of [3] extend the idea of CSN by two principles. First, they allow subspaces in layers (with different weights) to share knowledge between subspaces additionally besides tasks. Naturally, this extends the **alpha units** by the number of subspaces, e.g., for two tasks (A and B) and two subspaces (1 and 2) the α matrix is $\mathbb{R}^{4 \times 4}$ as given in the following equation:

$$\begin{bmatrix} \tilde{h}_{A_1,l}^T \\ \dots \\ \tilde{h}_{B_2,l}^T \end{bmatrix} = \begin{bmatrix} \alpha_{A_1 A_1} & \dots & \alpha_{B_2 A_1} \\ \vdots & \ddots & \vdots \\ \alpha_{A_1 B_2} & \dots & \alpha_{B_2 B_2} \end{bmatrix} [h_{A_1,l}^T \dots h_{B_2,l}^T],$$

where $\alpha_{A_1 B_2}$ refers to the alpha value of subspace one of task A and subspace two of task B . The output $[\tilde{h}_{A_1,l}^T, \dots, \tilde{h}_{B_2,l}^T]^T$ is the input to the next layer.

Further, the sluice network makes use of skip layers for the final prediction. Therefore, the results $\tilde{h}_{t,l}$ of each task t and layer l are concatenated in a matrix. Through a linear combination of this matrix with the so-called **beta unit**, the calculation results in the final task specific output, similar to the beta unit of the ERN shown in Fig. 1. Again, the supervised training learns the values of the beta-unit automatically.

E. Emerging Relation Network

Inspired by the work of [2], [3], we replace the subspace based sharing mechanism of SNs with a per neuron based sharing mechanism in the **alpha unit**. Therefore, a matrix, where each dimension is equal to the summed number of neurons across all tasks at a layer i replaces the alpha unit. This results in the following exemplarily calculation for two tasks with m and n neurons at layer l , respectively:

$$\begin{bmatrix} \tilde{h}_{1,l}^T \\ \tilde{h}_{2,l}^T \end{bmatrix} = \begin{bmatrix} \alpha_{1,1} & \dots & \alpha_{1,n} \\ \dots & \dots & \dots \\ \alpha_{m,1} & \dots & \alpha_{m,n} \end{bmatrix} [h_{1,l}^T \ h_{2,l}^T], \quad (2)$$

where $\alpha_{m,n}$ refers to neuron m of the first task and neuron n to the second task, $h_{1,l}$ is of size m , and $h_{2,l}$ of size n , respectively.

In our intuition, this provides the learning procedure to learn relevant relations between tasks without restrictions of the subspaces. Additionally, this mechanism avoids selecting the hyperparameter for the number of subspaces. Ideally, during the learning procedure, neurons or groups of neurons emerge that benefit from one task to one or more tasks. In the schematic overview in Fig. 1, the exemplary weights show such a learned relation through the heatmap. In this heatmap, one group has negative weights; another group has positive weights, while others are around zero, hence, sharing no information.

Note that this extension increases the number of parameters for the network. The additional parameters increase with

an increasing number of tasks, layers, and neurons in each layer. However, it avoids selecting the additional subspace hyperparameter present in the SN.

IV. EXPERIMENTAL EVALUATION

This section evaluates the experiments:

- to quantify the improvement of deep learning based MTL architectures compared to STL models,
- to evaluate the task embedding for MLP, and
- to evaluate the ERN against the SN.

Therefore, we first give details on the design of the experiments, followed by the evaluation. Finally, we discuss the key results.

A. Design of Experiments

In our experiments, we compare a STL model for each park against different MTL approaches. In particular, we evaluate the task embedding (MLPWP), an MLP without the task embedding (MLPNP), an HPS architecture, a CSN, and an SN. Finally, we evaluate our introduced ERN. All networks include temporal information (e.g., hour of the day) via an embedding layer to incorporate information relevant for the time series forecast. As a baseline, we use the single-park MLP that also utilizes an embedding layer to consider the temporal information.

1) *Data*: In our experiments, we used a solar and a wind park dataset. The solar dataset consists of 23 parks, while the wind dataset consists of 15 parks. In this scenario, a task corresponds to the prediction of the generated power of a single park. Ideally, information sharing within the MTL setting allows improving the overall forecast error across all tasks.

By making use of two datasets with different kinds of features and target variables, we show the strengths and weaknesses of the evaluated algorithms. In both datasets, the uncertainty of the NWP makes it challenging to predict the generated power. As weather forecasts are valid for a larger area (a so-called grid-size of 2.8 km), a mismatch between the forecast position and the actual placement of a park causes uncertainty. Further, the uncertainty increases with an increasing forecast horizon of the weather prediction [26].

The solar dataset has data from the beginning of 2015 till the end of April 2016. The wind dataset covers the years 2015 and 2016. In both cases, the year 2016 is used as the test dataset. 80% of the shuffled data from the year 2015 is used as a training dataset and 20% is used to find hyperparameters.

Each park in both datasets is standardized based on the training dataset. By merging data from parks by their timestamps, we assure that information between tasks relate and we neglect non-overlapping timestamps. As weather forecasts are only available in an hourly resolution, while the generated power is available in a 15 minute resolution, the input features are linearly interpolated, resulting in four times more data samples per park. All in all, this preprocessing results in 24328 samples per park for training and validation for the wind dataset and 23040 samples for testing. For the solar dataset, 24796 samples

are used for training and validation and 8396 samples for testing.

The solar dataset is generally considered a more straightforward problem compared to the wind park dataset. The relation between the input feature radiation and the generated power is mostly linear. However, weather features influence each other non-linearly, making it still a challenging problem. The solar dataset contains the following features: Temperature (at height 2 m), geopotential, total surface cloud coverage, albedo surface, total surface precipitation, snow surface density, snow depth surface water equivalent, snow surface depth, mean diffuse and direct short wave surface radiation, direct radiation, diffuse radiation, radiation aggregated. To improve the forecast quality, we add so-called time-shifted features from one hour in the past as well as one from the future from influencing weather features [27]. For the solar dataset, we included in those sliding windows the following features: Direct and diffuse short wave radiation.

The wind dataset contains the following features: wind speed and wind direction (at height 32 m, 73 m, 122 m), air pressure, temperature (at height 36 m, 122 m), relative humidity, unreduced ground pressure, pressure reduced, geopotential, and total precipitation. Compared to the solar dataset, this dataset is more challenging as the relation between wind and the generated power is highly non-linear. For the wind dataset, we included time-shifted features for all wind speeds and wind directions at different heights.

Further, we extracted the following temporal information (for both datasets) from the timestamps for all tasks: Hour of the day, week of the year, and day of the month. As stated previously, encodes those features as input.

2) *Hyperparameters*: To ensure comparable network sizes, we follow the same principle for all networks. The first hidden layer size is equal to the number of input features multiplied by 10. Note that initially transforming the input features in a higher-dimensional space typically improves the performance [28]. Afterward, in each layer, the number of neurons is reduced by 50% to a minimum of 5 neurons before the output.

For HPS networks, we include two task specific layers with sizes 5 and 1. Utilizing Xavier as initialization, as a state-of-the-art method to initialize weights, we minimize the risk of exploding gradients [29]. We initialize alpha units with 0.9 on the diagonal and $0.1/n$, where n refers to the number of elements without the diagonal. This balanced initialization assures that initially, tasks (CSN), subspaces (SN), or neurons (ERN) have a large weight with themselves. Information between tasks, etc., have an initially smaller weight, hence sharing less information.

After each layer, except the output layer, we include (in the following order) a leaky rectified linear unit (with a slope of 0.01), a batch normalization layer, and 50% dropout. For all embedding layers, we include a dropout of 25%.

For MTL networks and the MLP for each park, we use a batch size of 512. In the case we train a MLP to forecast all parks, we use a batch size of 2048 to reduce computational

effort as the number of samples increases. To accelerate the training, we train for 20 epochs with a one-cycle learning rate scheduler [30] with a maximum learning rate of 0.01 and cosine annealing. To finetune the weights, we conclude the training with 100 epochs and a small learning rate of $1e^{-4}$. In all epochs, we shuffle the training data. As training library we used *pytorch* [31] and *fastai* [32].

3) *Significance Test and Skill Score*: In the final results, we compare the forecast errors of each model and each park to baseline based on the root mean squared error (RMSE) on the test data. On the solar dataset, we utilize the *Wilcoxon signed-rank test* to show the significance of our models against the baseline. As the wind dataset has only 15 tasks and the Wilcoxon signed-rank test requires a sample size larger than 20 [33], we rely on a t-test. Therefore, we test the differences between a model and the baseline for normality with the *Shapiro-Wilk* test beforehand. In all hypothesis tests, we use a confidence level of $\alpha = 0.01$.

To get insights into the amount of improvement, we use a mean skill score across all parks given by the following equation:

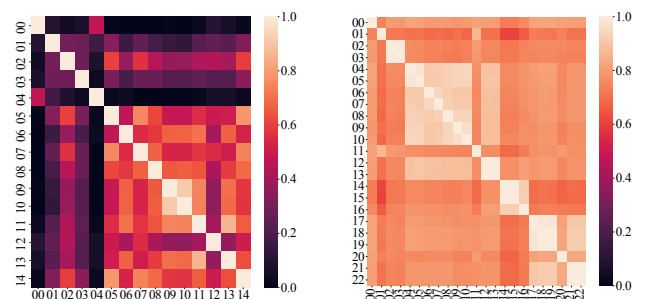
$$\text{SkillScore} = \frac{1}{k} \sum_{k=1}^{k=K} 1 - \frac{RMSE_{ref_k}}{RMSE_{baseline_k}}, \quad (3)$$

where $k \in 1, \dots, K$ refers to the current park, $RMSE_{ref_k}$ and $RMSE_{baseline_k}$ are the RMSE of the reference model and the baseline.

B. Experimental Results

This section details the evaluation results on the wind and the solar dataset described before. As pointed out in the previous section, we train and evaluate several multi-task models on both datasets and compare it to the baseline. Note that the asterisk symbol marks significantly different models compared to the baseline.

To get an initial impression on how different tasks relate to each other, we calculate the Pearson correlation on the training



(a) Pearson correlation coefficient between power generation of wind parks. (b) Pearson correlation coefficient between power generation of solar parks.

Fig. 3: Pearson correlation coefficient of power generation for wind and solar parks calculated based on training and validation data.

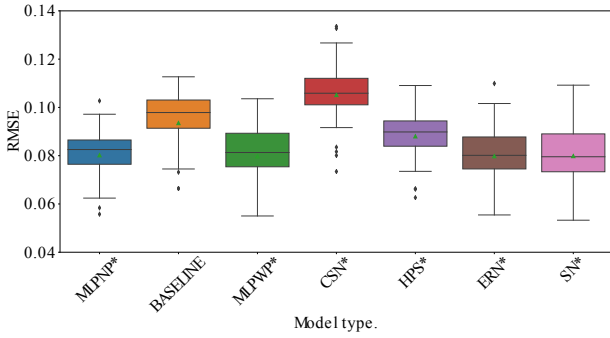


Fig. 4: Evaluation results for the solar dataset. The asterisk symbol marks significantly different models compared to the baseline. Triangles indicate the mean. The boxplots include the following models: An MLP without task embedding (MLPNP), the STL baseline, an MLP with task embedding (MLPWP), the cross-stitch network (CSN), the hard parameter sharing network (HPS), the emerging relation network (ERN), and the sluice network (SN).

and validation data for the target variable between the different tasks. Fig. 3 summarizes those results. For the wind dataset, the Pearson correlation is between 0 and 1. In Fig. 3a, at least six parks have a correlation below 0.4. In the case of solar parks in Fig. 3b, the correlation for all parks is between 0.6 and 1, indicating a higher correlation in contrast to the wind parks.

Fig. 4 summarizes the evaluation results for the solar dataset. The task embedding improves the forecast error compared to the baseline. The CSN has a significantly worse error compared to the baseline. The SN model improves the quality of the forecast significantly and has, among all models, one of the best performances. The proposed ERN also gives substantially better results than the STL baseline. All models, except MLPWP and the SN, have outliers

More detailed results for each park are given in Table I. The table presents the RMSE for each park and model and highlights the best one in bold. Results are summarized through the mean skill score at the end of the table compared to the baseline. Interestingly, the task embedding model yields the best results regarding the skill score. In particular, the model has an improvement of 14.96%. The MLPNP model, without the additional task embedding, has a lower improvement of 14.1%. The HPS architecture has among the smallest improvement with 5.73%. The SN model has an improvement of 14.85%. Finally, the ERN has a skill score of 14.77%.

Fig. 5 summarizes results on the wind park dataset. The CSN is worse than the baseline. Our approach, the ERN model, outperforms the baseline and has two outliers. All other models are not statistically different from the baseline.

Table II details the results from the boxplot. For ten parks, the ERN achieves the best results resulting in an overall improvement of 7.74%. The SN has a small improvement of 3.54%; however, this result is not significant. All other models

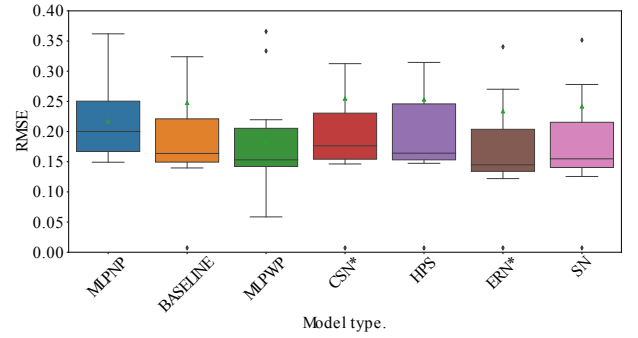


Fig. 5: Evaluation results for the wind dataset. The asterisk symbol marks significantly different models compared to the baseline. Triangles indicate the mean. The boxplots include the following models: An MLP without task embedding (MLPNP), the STL baseline, an MLP with task embedding (MLPWP), the cross-stitch network (CSN), the hard parameter sharing network (HPS), the emerging relation network (ERN), and the sluice network (SN).

have a negative skill score and are not significantly better than the baseline. Also note, that the RMSEs of most models for *ParkWind05* are rather large and indicate an outlier.

C. Discussion

Generally, in our results, we can see that MTL architectures improve upon a STL model of similar model size. Depending on the dataset and the model, the results vary. For solar dataset, the task embedding leads to the best improvement in terms of the skill score. This result is partly surprising as it is considered an HPS network forcing the learning process to learn a common representation instead of a task specific one. However, most solar parks have a high Pearson correlation, see Fig. 3b. This strong correlation is probably beneficial for a common representation across all tasks resulting in the best results. The results of the MLPNP also support this observation. The mean skill score of above 14% suggests that the data augmentation through combined training of all tasks already improves upon the STL architecture for the solar dataset even without task specific information or layers.

Results of the SPS architectures, except the CSN, lead to a significant improvement compared to the baseline. However, the mean skill score is slightly worse compared to the task embedding architecture. The improvement of SN and ERN are of similar magnitude. Suggesting that it is beneficial to utilize the ERN to avoid selection of the subspace hyperparameter of the SN.

In the wind dataset, only the SN achieves a significant improvement upon the STL baseline. This effect is explainable by the loosely related tasks, see Fig. 3a. During training, the neuron based sharing mechanism allows the ERN to learn a representation and a sharing mechanism that is beneficial for the small correlation between tasks automatically. The SN results could potentially improve with a different number

TABLE I: RMSE results for each park and model for the solar dataset. The asterisk symbol marks significantly different models compared to the baseline. The table includes the following models: An MLP without task embedding (MLPNP), the STL baseline, an MLP with task embedding (MLPWP), the cross-stitch network (CSN), the hard parameter sharing network (HPS), the emerging relation network (ERN), and the sluice network (SN).

ParkName	BASELINE	CSN*	ERN*	HPS*	MLPNP*	MLPWP*	SN*
ParkPV00	0.0912	0.1051	0.0738	0.0829	0.0767	0.0799	0.0781
ParkPV01	0.0732	0.0835	0.0572	0.0735	0.0584	0.0552	0.0533
ParkPV02	0.0982	0.1023	0.0801	0.0888	0.0842	0.0852	0.0834
ParkPV03	0.0950	0.1327	0.0774	0.0883	0.0771	0.0775	0.0749
ParkPV04	0.0745	0.0817	0.0587	0.0661	0.0627	0.0631	0.0609
ParkPV05	0.1039	0.1090	0.0838	0.0942	0.0854	0.0897	0.0894
ParkPV06	0.0988	0.1115	0.0916	0.0929	0.0876	0.0877	0.0933
ParkPV07	0.0664	0.0734	0.0554	0.0626	0.0557	0.0550	0.0544
ParkPV08	0.0937	0.0999	0.0763	0.0849	0.0798	0.0807	0.0796
ParkPV09	0.0664	0.0916	0.0639	0.0663	0.0732	0.0607	0.0633
ParkPV10	0.1009	0.1059	0.0813	0.0926	0.0825	0.0820	0.0788
ParkPV11	0.1028	0.1067	0.0822	0.0946	0.0841	0.0895	0.0847
ParkPV12	0.0979	0.1139	0.0827	0.0909	0.0835	0.0866	0.0839
ParkPV13	0.0962	0.1028	0.0752	0.0898	0.0783	0.0766	0.0745
ParkPV14	0.1058	0.1186	0.0916	0.1070	0.0972	0.0891	0.0886
ParkPV15	0.1127	0.1335	0.1099	0.1091	0.1027	0.1036	0.1092
ParkPV16	0.0943	0.1126	0.0756	0.0888	0.0762	0.0742	0.0722
ParkPV17	0.1039	0.1057	0.1016	0.1016	0.0999	0.0951	0.1019
ParkPV18	0.0915	0.1031	0.1012	0.0894	0.0783	0.0786	0.0982
ParkPV19	0.1013	0.1267	0.0862	0.0935	0.0875	0.0903	0.0884
ParkPV20	0.1047	0.1105	0.0893	0.0975	0.0906	0.0932	0.0905
ParkPV21	0.0746	0.0801	0.0608	0.0760	0.0624	0.0584	0.0570
ParkPV22	0.1033	0.1079	0.0794	0.0949	0.0856	0.0813	0.0780
SkillScore	0.0000	-0.1281	0.1477	0.0573	0.1410	0.1496	0.1485

TABLE II: RMSE results for each park and model for the wind dataset. The asterisk symbol marks significantly different models compared to the baseline. The table includes the following models: An MLP without task embedding (MLPNP), the STL baseline, an MLP with task embedding (MLPWP), the cross-stitch network (CSN), the hard parameter sharing network (HPS), the emerging relation network (ERN), and the sluice network (SN).

ParkName	BASELINE	CSN*	ERN*	HPS	MLPNP	MLPWP	SN
ParkWind00	0.1633	0.1749	0.1330	0.1622	0.1710	0.1503	0.1476
ParkWind01	0.1553	0.1558	0.1592	0.1578	0.2047	0.1559	0.1640
ParkWind02	0.2054	0.2103	0.1737	0.1978	0.2235	0.1919	0.1943
ParkWind03	0.1637	0.1763	0.1448	0.1641	0.1766	0.1531	0.1493
ParkWind04	0.2858	0.2956	0.2701	0.2879	0.2412	0.2006	0.2780
ParkWind05	1.2202	1.2266	1.2083	1.2384	0.3620	0.3658	1.2090
ParkWind06	0.1647	0.1772	0.1376	0.1623	0.1730	0.1525	0.1548
ParkWind07	0.1397	0.1463	0.1386	0.1473	0.1491	0.1421	0.1448
ParkWind08	0.1541	0.1732	0.1351	0.1687	0.1629	0.1420	0.1360
ParkWind09	0.0072	0.0071	0.0071	0.0070	0.2001	0.0586	0.0072
ParkWind10	0.3240	0.3125	0.3404	0.3146	0.3314	0.3335	0.3515
ParkWind11	0.2271	0.2377	0.1928	0.2214	0.2595	0.2101	0.2132
ParkWind12	0.1426	0.1502	0.1220	0.1483	0.1510	0.1344	0.1255
ParkWind13	0.2150	0.2233	0.2147	0.2702	0.2994	0.2196	0.2175
ParkWind14	0.1446	0.1525	0.1271	0.1485	0.1497	0.1340	0.1312
SkillScore	0.0000	-0.0409	0.0774	-0.0256	-1.8287	-0.3790	0.0354

of subspaces. However, this would require a hyperparameter search, which the sharing mechanism of the ERN avoids.

V. CONCLUSION AND FUTURE WORK

In our article, we successfully showed the improvement of MTL architectures upon STL models. Therefore, we quantified the improvement employing the mean skill score based on the RMSE for a solar and wind park dataset. We also showed their significance against an MLP baseline for each park. Further,

we suggest two new architectures that help in tackling different challenges in MTL predictions.

The task embedding architecture provides a simple and effective method when tasks are strongly correlated and a common representation is beneficial. In contrast to SPS architectures, this HPS model limits the number of required parameters while achieving the best significant results on the solar dataset. As complex models require extensive computational resources and are contrary to climate goals [7], the task embedding provides a robust model that improves the

forecast error while minimizing the computational effort.

The proposed adaptation of the SN through a per neuron based sharing mechanism allows the ERN to achieve results of similar magnitude on the solar dataset compared to the task embedding and the SN. Results on the wind dataset show that the automatic learning process is superior compared to its predecessor, the SN, as it is the only one improving upon the baseline on the wind dataset.

A future goal is to incorporate additional data for the solar dataset to increase the expressiveness of the results. Further, we aim at utilizing the learned knowledge from MTL architectures for predictions of parks with limited historical data.

ACKNOWLEDGMENT

This work was supported within the project Prophecy (0324104A) funded by BMWi (Deutsches Bundesministerium für Wirtschaft und Energie / German Federal Ministry for Economic Affairs and Energy).

REFERENCES

- [1] S. Ruder, "An Overview of Multi-Task Learning in Deep Neural Networks," *CoRR*, p. 14, 2017, arXiv: 1706.05098.
- [2] I. Misra, A. Shrivastava, A. Gupta, and M. Hebert, "Cross-Stitch Networks for Multi-task Learning," in *Proceedings of the IEEE Computer Society Conference on Computer Vision and Pattern Recognition*, 2016, pp. 3994–4003.
- [3] S. Ruder, J. Bingel, I. Augenstein, and A. Søgaard, "Latent Multi-Task Architecture Learning," *Proceedings of the AAAI Conference on Artificial Intelligence*, vol. 33, pp. 4822–4829, 2019.
- [4] M. Lange and U. Focken, "Overview of Wind Power Prediction Systems," in *Physical Approach to Short-Term Wind Power Prediction*. Springer-Verlag, 2006, pp. 7–22.
- [5] J. Henze, J. Schreiber, and B. Sick, "Representation Learning in Power Time Series Forecasting," in *Deep Learning: Algorithms and Applications*. Springer, Cham, 2020, pp. 67–101.
- [6] "Windenergie Report Deutschland 2017," 2018, Fraunhofer Institut für Energiewirtschaft und Energiesystemtechnik.
- [7] R. Schwartz, J. Dodge, N. A. Smith, and O. Etzioni, "Green AI," *CoRR*, 2019, arXiv: 1907.10597.
- [8] M. Long, Z. Cao, J. Wang, and P. S. Yu, "Learning Multiple Tasks with Multilinear Relationship Networks," in *Advances in Neural Information Processing Systems 30 (NIPS)*, 2017, pp. 1594–1603.
- [9] Y. Lu, A. Kumar, S. Zhai, Y. Cheng, T. Javidi, and R. Feris, "Fully-adaptive feature sharing in multi-task networks with applications in person attribute classification," in *Proceedings - 30th IEEE Conference on Computer Vision and Pattern Recognition, CVPR 2017*, vol. 30. Institute of Electrical and Electronics Engineers Inc., 2017, pp. 1131–1140.
- [10] A. Søgaard and Y. Goldberg, "Deep multi-task learning with low level tasks supervised at lower layers," in *Proceedings of the 54th Annual Meeting of the Association for Computational Linguistics (Volume 2: Short Papers)*. Association for Computational Linguistics, 2016, pp. 231–235.
- [11] K. Hashimoto, C. Xiong, Y. Tsuruoka, and R. Socher, "A Joint Many-Task Model: Growing a Neural Network for Multiple {NLP} Tasks," in *Proceedings of the 2017 Conference on Empirical Methods in Natural Language Processing*. Association for Computational Linguistics, 2017, pp. 1923–1933.
- [12] R. Cipolla, Y. Gal, and A. Kendall, "Multi-task Learning Using Uncertainty to Weigh Losses for Scene Geometry and Semantics," in *Proceedings of the IEEE Computer Society Conference on Computer Vision and Pattern Recognition*. IEEE Computer Society, 2018, pp. 7482–7491, arXiv: 1705.07115.
- [13] Y. Zhang and Q. Yang, "A Survey on Multi-Task Learning," *CoRR*, p. 20, 2017, arxiv: 1707.08114.
- [14] K. A. Ming Chai Christopher K I Williams Stefan Klanke Sethu Vijayakumar, "Multi-task Gaussian Process Learning of Robot Inverse Dynamics," in *Advances in Neural Information Processing Systems 21*, 2009, pp. 265–272.
- [15] B. Rakitsch, C. Lippert, K. Borgwardt, and O. Stegle, "It is all in the noise: Efficient multi-task Gaussian process inference with structured residuals," in *Advances in Neural Information Processing Systems 26*, 2013, pp. 1466–1474.
- [16] K. A. Ming Chai, "Generalization Errors and Learning Curves for Regression with Multi-task Gaussian Processes," in *Advances in Neural Information Processing Systems 22*, 2009, pp. 279–287.
- [17] Y. Zhang and D. Y. Yeung, "Semi-supervised multi-task regression," in *ECML PKDD 2009: Machine Learning and Knowledge Discovery in Databases*, vol. 5782 LNAI, no. PART 2. Springer, Berlin, Heidelberg, 2009, pp. 617–631.
- [18] A. C. Lozano and G. Swirszcz, "Multi-Level Lasso for Sparse Multi-Task Regression," in *Proceedings of the 29th International Conference on International Conference on Machine Learning*, 2012, pp. 595–602.
- [19] S. Kim and E. P. Xing, "Tree-Guided Group Lasso for Multi-Task Regression with Structured Sparsity," in *Proceedings of the 27th International Conference on International Conference on Machine Learning*, ser. ICML, 2010, pp. 543–550.
- [20] P. Rai, A. Kumar, and H. Daumé III, "Simultaneously Leveraging Output and Task Structures for Multiple-Output Regression," in *Advances in Neural Information Processing Systems 25*, 2012, pp. 3185–3193.
- [21] Z. Tan, G. De, M. Li, H. Lin, S. Yang, L. Huang, and Q. Tan, "Combined electricity-heat-cooling-gas load forecasting model for integrated energy system based on multi-task learning and least square support vector machine," *Journal of Cleaner Production*, vol. 248, p. 119252, 2020.
- [22] P. Huang, C. Wen, L. Fu, Q. Peng, and Y. Tang, "A deep learning approach for multi-attribute data: A study of train delay prediction in railway systems," *Information Sciences*, vol. 516, pp. 234–253, 2020.
- [23] H. Liu, Q. Li, and Y. Gu, "A multi-task learning framework for gas detection and concentration estimation," *Neurocomputing*, 2020.
- [24] M. Dorado-Moreno, N. Navarin, P. A. Gutiérrez, L. Prieto, A. Sperduti, S. Salcedo-Sanz, and C. Hervás-Martínez, "Multi-task learning for the prediction of wind power ramp events with deep neural networks," *Neural Networks*, vol. 123, pp. 401–411, 2020.
- [25] S. Vogt, A. Braun, J. Dobschinski, and B. Sick, "Wind Power Forecasting Based on Deep Neural Networks and Transfer Learning," in *18th Wind Integration Workshop*, 2019, p. 8.
- [26] J. Schreiber, A. Buschin, and B. Sick, "Influences in Forecast Errors for Wind and Photovoltaic Power: A Study on Machine Learning Models," in *INFORMATIK 2019: 50 Jahre Gesellschaft für Informatik*, K. David, K. Geihs, M. Lange, and G. Stumme, Eds. Gesellschaft für Informatik e.V., 2019, pp. 585–598.
- [27] J. Schreiber and B. Sick, "Quantifying the Influences on Probabilistic Wind Power Forecasts," in *ICPRE*, vol. 3, 2018, p. 6.
- [28] S. R. Sain and V. N. Vapnik, *The Nature of Statistical Learning Theory*. Springer-Verlag New York, 2006, vol. 38, no. 4.
- [29] X. Glorot and Y. Bengio, "Understanding the difficulty of training deep feedforward neural networks," *AISiats*, vol. 9, pp. 249–256, 2010.
- [30] L. N. Smith, "A Disciplined Approach To Neural Network Hyper-Parameters: Part 1," *CoRR*, pp. 1–21, 2016, arXiv: 1803.09820.
- [31] A. Paszke, S. Gross, F. Massa, A. Lerer, J. Bradbury, G. Chanan, T. Killeen, Z. Lin, N. Gimselshein, L. Antiga, A. Desmaison, A. Kopf, E. Yang, Z. DeVito, M. Raison, A. Tejani, S. Chilamkurthy, B. Steiner, L. Fang, J. Bai, and S. Chintala, "Pytorch: An imperative style, high-performance deep learning library," in *Advances in Neural Information Processing Systems 32*, H. Wallach, H. Larochelle, A. Beygelzimer, F. d'Alché-Buc, E. Fox, and R. Garnett, Eds. Curran Associates, Inc., 2019, pp. 8026–8037.
- [32] "Fastai python library v1.2," <http://docs.fast.ai/>, 2020, [Online; accessed 2020-04-01].
- [33] F. Pedregosa, G. Varoquaux, A. Gramfort, V. Michel, B. Thirion, O. Grisel, M. Blondel, P. Prettenhofer, R. Weiss, V. Dubourg, J. Vanderplas, A. Passos, D. Cournapeau, M. Brucher, M. Perrot, and E. Duchesnay, "Scikit-learn: Machine learning in Python," *JMLR*, vol. 12, pp. 2825–2830, 2011.